International Journal of Thermophysics, Vol. 17, No. 4, 1996

Compressibilities of Ternary Mixtures C_1–nC_{16}–CO_2 Under Pressure from Ultrasonic Measurements of Sound Speed

J. L. Daridon,[1,2] B. Lagourette,[1] and P. Labes[1]

Received November 21, 1995

Speed of sound measurements have been performed on three mixtures of the ternary system methane + carbon dioxide + normal hexadecane. The systems have been investigated from 12 to 70 MPa in the temperature range from 313 to 393 K. Furthermore, these measurements have allowed the evaluation of the isothermal and the isentropic compressibilities up to 70 MPa from low pressure (<40-MPa) density data.

KEY WORDS: compressibility; equation of state; high pressure; speed of sound.

1. INTRODUCTION

To assess the quantity and quality of petroleum reserves in an oil field, to optimize recovery, and to select and install the appropriate equipment, the petroleum industry uses a number of thermodynamic models within numerical simulators. The development and improvement of these models depend closely on the reliability and diversity of the experimental data on which their respective adjustments are based. In particular, it is important to possess experimental information covering the pressure conditions encountered at all stages in petroleum production. While for most of the pure substances involved in the composition of crude oils, measurements of volumetric, calorimetric, and phase equilibrium properties have been conducted under pressure, such data remain scarce for synthetic mixtures. Moreover, when studies of this kind have been carried out, they generally

[1] Laboratoire Haute Pression, Centre Universitaire de Recherche Scientifique, Université de Pau, Avenue de l'Université, 64000 Pau, France.
[2] To whom correspondence should be addressed.

0195-928X/96/0700-0851$09.50/0

concern either only one physical property or only one composition. And yet it is essential to develop and test the mixing rules used in the thermodynamic models, to possess a wide range of data.

Our research has been conducted within this context. The purpose of this paper is to contribute original experimental data on three mixtures of the ternary system methane–hexadecane–carbon dioxide, which is of evident interest in the field of petroleum simulation. More precisely, ultrasonic measurements of speed of sound were carried out in the pressure range 0.1–70 MPa and in the temperature range 293–393 K to complete the study of this system, which has already been investigated [1] as regards determinations of saturation curves (using a full-visibility PVT cell within the interval 0.1–50 MPa) and measurements of density using an Anton Paar (DMA 512) densimeter up to 40 MPa. Measurement of the speed of propagation of ultrasound waves u is of interest from a thermodynamic point of view if it coincides perfectly with the speed of sound within the low-frequency limit c. Under these conditions ultrasonic speed is a purely thermodynamic property connected with a reversible adiabatic process and the corresponding data can be used to determine the isentropic compressibility coefficient β_S through the following thermodynamic relationship:

$$\beta_S = \frac{1}{\rho u^2} \tag{1}$$

provided the density ρ of the fluid is known, along with the speed u, under the same pressure and temperature conditions. However, it can occur that the pressure ranges for which information on ρ and u are available do not match precisely. This is particularly the case, in this study, as a result of the nonoverlap of the pressure operating ranges of the ultrasound apparatus and the densimeter. In order to get around this limitation, we use a calculation procedure to predict the adiabatic and isothermal compressibility coefficients of the sample, based on the combination of sound speed data and knowledge of the density. It is worth recalling, on the subject of coefficients (which are difficult to obtain experimentally), that they are essential for the calculation of compression ratios for turboexpanders and other compressors, as well as for simulation of phenomena taking place at the level of chokes and in the reservoir itself.

2. EXPERIMENTAL TECHNIQUE

The apparatus used to determine the velocities is operational at high pressures and has been described in detail by Ye et al. [2]. The principle

is based on a method of transmission of ultrasonic pulses (frequency: 2 MHz) through the sample. The pulses are short in duration (5 μs) and are repeated every 5 ms. Evaluation of the time interval separating the selected echoes is achieved by the well-known pulse–echo–overlap method [3]. Based on the cumulative errors connected with uncertainties in the temperature, the pressure, and the measurement of time intervals, the accuracy of the measurements is within 0.2% over the entire pressure range. The fluid samples are placed in a cylindrical autoclave cell in which they occupy a space bounded transversally by two metal buffers, at the end of which the transmitter and receiver transducers (Quartz and Silice brand piezoelectric ceramic) are mounted. The samples are brought under pressure and the pressure is maintained by a mercury volumetric pump (in which the purity of mercury used is better than 99.9%). The temperature is regulated by oil circulating in an annular space between the main body of the cell and a Teflon casing which serves as a heat insulator around the autoclave part. A double-insulated and tight electrical passage [4, 5] fitted in the cell enables detection of the P, T conditions within the sample itself.

3. MEASUREMENTS

The investigations were carried out on three mixtures (Table I) of the ternary system composed of carbon dioxide, methane, and normal hexadecane under pressure and temperature conditions compatible with the liquid state. The ternary mixtures were prepared by weighing, the hexadecane being introduced first in the liquid state and the two other components being transferred in the gaseous state under controlled conditions of pressure and temperature. The degrees of purity of the chemicals used are better than 99.5% for the linear hexadecane (Sigma) and better than 99.9% for the methane and carbon dioxide (supplied by AGA GAZ).

The ultrasonic speed experiments were conducted at a fixed temperature and variable pressure in steps of the order of 2 MPa from an upper pressure of 70 MPa down to a pressure as close as possible to the bubble pressure. The values of u are presented in Tables II to IV and some are shown in Figs. 1 and 2. These figures characterize the networks of

Table I. Composition of the Mixtures

Ternary	x_{CO_2}	x_{C_1}	$x_{n\text{-}C_{16}}$
a	0.12	0.10	0.78
b	0.10	0.46	0.44
c	0.44	0.11	0.45

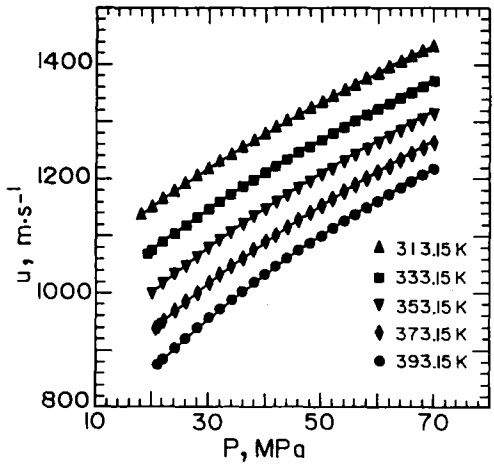

Fig. 1. Experimental sound speed in mixture b as a function of pressure.

isothermal and isobaric curves defined within the limits of the temperature and pressure intervals studied. On the $U(P)$ diagram we have indicated the liquid–vapor equilibrium line for the mixture studied in order to be able to situate the P and T range in which the ultrasonic speed investigation was conducted with respect to that line. In agreement with the usual observations for the liquid state, the above groups of curves are regular and correspond to pressure coefficients $(\partial U/\partial P)_T$ and temperature coefficients $(\partial U/\partial P)_P$ which are >0 and <0, respectively.

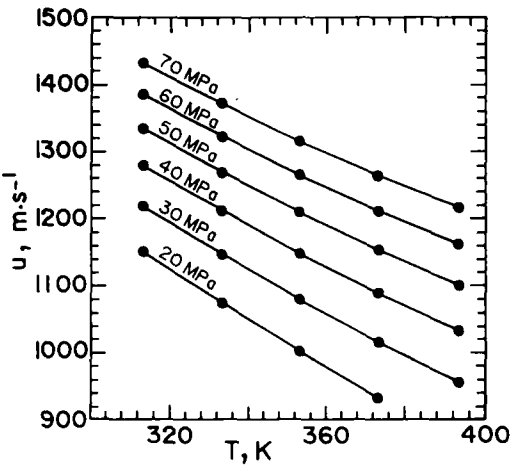

Fig. 2. Experimental sound speed in mixture b as a function of temperature.

Table II. Experimental Values of the Sound Speed in Mixture a

	$U(\mathrm{m \cdot s^{-1}})$ at T(K)			
P(MPa)	313.15	333.15	353.15	373.15
70	1554.5	1498.4	1446.1	1397.9
68	1546.5	1490.5	1438.0	1389.2
66	1538.5	1482.1	1429.5	1380.5
64	1530.7	1474.1	1420.7	1371.4
62	1522.4	1465.5	1412.2	1362.7
60	1514.5	1456.7	1403.0	1353.1
58	1505.9	1448.0	1393.9	1344.0
56	1497.8	1439.5	1384.9	1334.6
54	1489.4	1430.6	1375.5	1324.8
52	1480.8	1421.5	1366.2	1315.3
50	1471.9	1412.6	1356.9	1305.0
48	1463.0	1403.1	1347.1	1295.1
46	1454.5	1394.0	1337.3	1284.9
44	1444.9	1384.6	1327.7	1274.7
42	1436.4	1375.0	1317.7	1264.0
40	1426.8	1365.2	1307.6	1253.6
38	1417.6	1355.4	1297.2	—
36	1408.1	1345.4	1286.8	—
34	1398.2	1335.1	1276.1	—
32	1388.3	1325.0	1265.1	—
30	1378.7	1314.6	1254.0	—
28	1368.5	1303.9	1242.8	—
26	1358.3	1293.1	1231.0	—
24	1347.6	1281.8	1219.2	—
22	1337.6	1270.8	1207.1	—
20	1326.7	1259.2	1195.2	—
18	1315.3	1242.7	1182.5	—
16	1304.2	1235.4	1170.2	—
14	1293.3	1223.3	1157.1	—
12	1281.0	1211.1	1143.5	—
10	1269.3	1197.9	1130.0	—
8	1257.4	1184.9	1115.4	—
6	1245.6	1171.5	1101.2	—
5	1239.0	1164.7	1094.0	—
4	1232.9	—	—	—

Table III. Experimental Values of the Sound Speed in Mixture b

	U (m·s^{-1}) at T (K)				
P (MPa)	313.15	333.15	353.15	373.15	393.15
70	1431.1	1371.1	1316.0	1264.5	1214.9
68	1422.1	1361.7	1306.3	1254.1	1204.7
66	1413.2	1352.3	1295.9	1243.4	1194.3
64	1403.5	1342.4	1285.9	1232.6	1183.0
62	1394.1	1332.7	1275.7	1222.1	1172.0
60	1384.5	1322.5	1265.1	1210.9	1160.2
58	1374.5	1312.1	1254.4	1199.9	1148.8
56	1364.7	1301.7	1243.5	1188.7	1137.4
54	1354.7	1291.0	1232.4	1177.2	1125.1
52	1344.3	1280.4	1221.2	1165.6	1113.2
50	1334.0	1269.3	1209.5	1153.3	1100.5
48	1323.4	1258.2	1197.8	1141.5	1087.7
46	1312.6	1248.8	1186.1	1129.0	1075.0
44	1301.8	1235.4	1173.6	1115.9	1061.3
42	1290.6	1223.4	1161.3	1103.8	1048.0
40	1279.4	1211.4	1148.9	1090.1	1033.9
38	1267.5	1199.0	1135.8	1076.1	1019.3
36	1256.0	1186.7	1122.4	1062.4	1004.6
34	1243.8	1173.7	1108.7	1047.4	988.9
32	1231.2	1160.5	1094.6	1032.3	973.5
30	1218.7	1147.0	1080.2	1017.4	956.8
28	1205.5	1132.9	1065.0	1001.3	940.0
26	1192.3	1118.8	1050.1	985.1	922.7
24	1178.5	1104.0	1034.1	967.8	904.0
22	1164.3	1088.6	1017.2	949.3	884.5
20	1149.9	1073.2	1000.4	931.0	—

4. APPLICATION OF SOUND SPEED DATA TO THE CALCULATION OF THERMOPHYSICAL PROPERTIES

It is possible to generate density data from speed of sound to an excellent degree of accuracy (of the order of 0.1%) by integrating the quantity $1/u^2$ (at constant temperature) with respect to pressure [6]. The basic relationship through which this operation can be carried out is

$$\rho(P, T) = \rho(P_i, T) + \int_{P_i}^{P} u^{-2}\, dP + T \int_{P_i}^{P} \alpha^2/C_P\, dP \tag{2}$$

The first integral term involved in Eq. (2) is evaluated directly from the speed of sound measurements. The second integral term, the value of which

Table IV. Experimental Values of the Sound Speed in Mixture c

	$U(\mathrm{m \cdot s^{-1}})$ at T(K)				
P(MPa)	313.15	333.15	353.15	373.15	393.15
70	1418.7	1358.0	1301.9	1250.1	1201.1
68	1410.0	1349.3	1292.9	1240.3	1191.4
66	1401.7	1340.4	1283.4	1230.8	1181.4
64	1392.8	1331.1	1273.7	1220.6	1171.0
62	1384.0	1321.7	1264.1	1210.7	1160.8
60	1375.2	1312.5	1254.2	1200.4	1150.0
58	1366.2	1303.2	1244.3	1190.1	1139.4
56	1353.9	1293.4	1234.3	1179.8	1128.2
54	1347.6	1283.6	1223.8	1168.9	1116.9
52	1338.1	1273.7	1213.6	1158.4	1105.6
50	1128.7	1263.6	1202.9	1146.9	1094.2
48	1318.9	1253.4	1192.1	1135.7	1082.0
46	1309.1	1243.0	1181.4	1124.2	1070.0
44	1299.1	1232.5	1169.9	1112.3	1057.8
42	1289.1	1221.6	1158.6	1100.6	1045.4
40	1278.6	1210.6	1147.1	1088.2	1032.2
38	1267.8	1199.5	1135.2	1075.7	1019.4
36	1257.4	1188.2	1123.1	1063.0	1005.7
34	1246.2	1176.4	1110.7	1049.6	991.7
32	1235.1	1164.6	1097.7	1036.2	977.9
30	1223.7	1152.6	1085.1	1022.2	963.1
28	1212.0	1140.1	1071.6	1008.1	947.5
26	1200.2	1127.2	1058.0	993.9	932.3
24	1188.0	1114.0	1043.6	978.5	915.3
22	1175.4	1100.5	1029.3	962.5	898.4
20	1163.0	1086.9	1014.7	946.1	881.0
18	1149.8	1072.5	999.0	928.9	862.5
16	1136.5	1058.0	983.0	911.6	843.2
14	1122.5	1042.8	965.9	892.7	822.7
12	1108.4	1026.9	948.6	—	—
10	1093.7	—	—	—	—

represents only a few percent of the first, can be calculated iteratively by Davis and Gordon's method [7] modified by Muringer et al. [8]. The procedure, which was developed to extend atmospheric pressure measurements on pure substances to high pressures, requires the further knowledge of $C_p(T)$, $\rho(T)$, and $\alpha(T)$ at a given initial pressure in order to begin the iterative process, a requirement which is not satisfied here. However, Daridon et al. [9] have proposed a method which can get around this

difficulty when density data at a few pressure values are available. This numerical method does, however, require that the conditions of measurement (pressure and temperature) of both properties (density and speed of sound) should be identical. As this is not the case here, we preferred to generate the missing data by means of a virial-type equation of state, involving 12 coefficients, which were recalculated for the occasion in such a way as to reproduce simultaneously and very accurately the experimental density data (up to 40 MPa) and all the sound speed measurements (up to 70 MPa). This coherent procedure of adjustment of an equation of state (used several times [10–12]) has the advantage that it is then possible to deduce by direct exploitation the values of ρ for any intermediate conditions along P and T up to 70 MPa as well as other derived thermophysical properties such as the compressibility coefficients β_T and β_S.

Our choice of equation of state was a modified Benedict–Webb–Rubin [13]—type formulation, more precisely the development adopted by Lee and Kesler [14] in their application of the principle of corresponding states with three parameters,

$$Z = 1 + \frac{B}{v} + \frac{C}{v^2} + \frac{D}{v^5} + \frac{c_4}{T^3 v^2}\left(\beta + \frac{\gamma}{v^2}\right)\exp\left(-\frac{\gamma}{v^2}\right) \tag{3}$$

in which Z represents the system's compressibility factor, defined by

$$Z = \frac{Pv}{RT} \tag{4}$$

and B, C, and D are three temperature-dependent parameters,

$$B = b_1 - \frac{b_2}{T} - \frac{b_3}{T^2} - \frac{b_4}{T^3} \tag{5}$$

$$C = c_1 - \frac{c_2}{T} + \frac{c_3}{T^3} \tag{6}$$

$$D = d_1 + \frac{d_2}{T} \tag{7}$$

The reason behind this selection is the very good predictive behavior of the Lee–Kesler model with respect to density and sound speed in the case of hydrocarbons. On several occasions we have been able to demonstrate its interesting potential, whether with gaseous-type mixtures [15–17] or liquid-type mixtures [18, 19].

The values of the parameters involved in Eqs. (3) to (7) were determined for each mixture in order to minimize the following objective function:

$$\mathrm{OBJ} = \frac{1}{N}\sum_{i=1}^{N}\frac{|u_{\mathrm{cal}_i} - u_{\mathrm{exp}_i}|}{u_{\mathrm{exp}_i}} + \frac{1}{M}\sum_{j=1}^{M}\frac{|\rho_{\mathrm{cal}_j} - \rho_{\mathrm{exp}_j}|}{\rho_{\mathrm{exp}_j}} \tag{8}$$

which corresponds to the double sum of the absolute deviations extended to all the density and sound speed measurements. The number of experimental data available for each of these two properties is different, and so each sum was divided by the number of measurements to avoid favoring thy prediction of one rather than the other of these physical properties. Moreover, as the experimental determinations of u and ρ are of the same order of accuracy (0.1 to 0.2%), it was not necessary to weight each relative deviation to allow for experimental error in each objective function. It should be emphasized that the only purpose of redefining the parameters, which was done for each mixture, and therefore for each composition, a, b, and c, is to develop a correlation able to adjust as precisely as possible both the density and the sound speed data measured in a pressure interval ranging from the mixture's saturation pressure to 70 MPa for temperatures between 293 and 373 K. Use of these new parameters must be restricted to this particular application.

Before applying this procedure to the three ternary mixtures, we decided to test its validity in the case of a pure substance (the results the procedure yielded with the ternaries will be presented later). For this purpose normal octane was used, because there are several speed of sound and density references available for this substance [20–22]. Moreover, we have already conducted measurements on octane in our laboratory [9] to test the reliability of our experimental apparatuses and of the numerical procedure developed subsequently. The intrinsic parameters of Eq. (3) were recalculated for octane, referring to the same measurements of u (performed along eight isotherms between 303 and 373 K for pressures between 20 and 100 MPa) and ρ (carried out at the same temperatures but at pressures limited to 40 MPa). In order to verify the validity of the new procedure, the values of density predicted up to 100 MPa by Eq. (3) were then compared with those calculated by the numerical procedure [9]. The maximum deviation observed between the two procedures was 0.2%. Similarly, comparison of the average absolute deviation ($=0.08\%$) and the average deviation ($=0.05\%$) failed to show the existence of any systematic error. Finally, it should be pointed out in Fig. 3, in which the deviation between the two numerical procedures is plotted, that the deviation does not increase systematically with pressure within the overall interval of the study

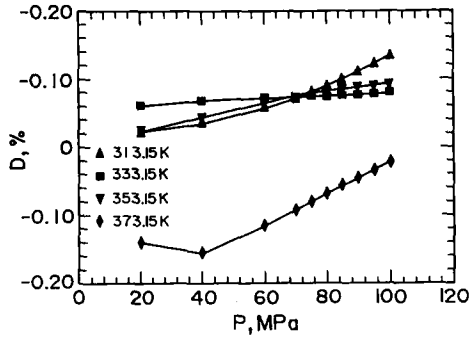

Fig. 3. Deviations between the densities calculated by the two procedures as a function of pressure.

(20–100 MPa). This comparative study performed on octane demonstrates that the procedure described in this paper provides results equivalent to those presented previously. However, it presents the added advantage that it can be implemented even if the conditions of measurement of the two properties at moderate pressures are dissimilar. Moreover, this procedure provides an equation of state which can be used to calculate u and ρ as well as the derived properties, β_T and β_S. In order to estimate the probable error on each calculated property, the effects on u, ρ, β_T, and β_S of performing the calculation with various perturbations on the input data are shown in Table V. It can be seen that the magnitude of the error on u and ρ is of the same order as the perturbation. But in the case of derived properties, particularly for β_T, the deviation is higher (1% in the most unfavorable case).

In the same way as for pure octane, the coefficients of the modified BWR equation were recalculated (Table VI) so as to provide the best predictions of the sound speed and the density for the three mixtures a, b, and c. The deviations observed point by point between the experimental data and the data calculated by Eq. (3) including these new parameters are represented as an illustration for mixture b in Figs. 4 and 5. These graphs show that the dispersion of errors appears random and that the deviations are not an increasing function of either temperature or pressure. To give a more general idea of the quality of the model, we indicate in Table VII, for each of the three systems, the average absolute deviation (percentage) and the maximum deviation (percentage) observed for the two properties considered (ρ and u). The values of these deviations show that the equation adjusted in this way yields a very good simultaneous prediction of sound speed (with a maximum error of the order of 0.2%) and density (maximum deviation of the order of 0.25%). Moreover, comparing average deviations

Table V. Effects on u, ρ, β_T, and β_S of Various Perturbations on the Input Data of Octane

Perturbation	Average absolute deviation (%)			
	u	ρ	β_S	β_T
u: random 0.2% ρ: random 0.2%	0.013	0.018	0.028	0.60
u: random 0.2% ρ: systematic 0.2%	0.018	0.22	0.22	0.57
u: systematic 0.2% ρ: random 0.2%	0.20	0.037	0.36	0.65
u: systematic 0.2% ρ: systematic 0.2%	0.20	0.15	0.55	1.0

Table VI. Parameters of Eq. (3), with T in K, P in Pa, and v in $m^3 \cdot mol^{-1}$

Parameter	Mixture a	Mixture b	Micture c
b_1	0.177546×10^{-02}	0.130827×10^{-02}	0.113462×10^{-02}
b_2	0.989923	0.392527	0.447762
b_3	$0.133046 \times 10^{+03}$	$0.889009 \times 10^{+02}$	$0.964131 \times 10^{+02}$
b_4	$0.225303 \times 10^{+06}$	$0.619888 \times 10^{+05}$	$0.660801 \times 10^{+05}$
c_1	0.208295×10^{-06}	0.367515×10^{-11}	0.679652×10^{-07}
c_2	0.412347×10^{-03}	0.107778×10^{-03}	0.116687×10^{-03}
c_3	$0.503269 \times 10^{+02}$	$0.578759 \times 10^{+01}$	$0.698066 \times 10^{+01}$
c_4	$0.242186 \times 10^{+03}$	$0.507699 \times 10^{+02}$	$0.546527 \times 10^{+02}$
d_1	0.100736×10^{-16}	0.107738×10^{-19}	0.667696×10^{-20}
d_2	0.392628×10^{-14}	0.557165×10^{-15}	0.650569×10^{-15}
β	0.514676	0.288073	0.363194
γ	0.298745×10^{-06}	0.974916×10^{-07}	0.107971×10^{-06}

Table VII. Comparison Between Experimental and Calculated Properties[a]

	Mixture a	Mixture b	Mixture c
AD% on u	-0.98×10^{-04}	-0.25×10^{-02}	-0.28×10^{-04}
AAD% on u	0.35×10^{-01}	0.42×10^{-01}	0.35×10^{-01}
MD% on u	0.10	0.15	0.17
AD% on ρ	-0.12×10^{-02}	0.12×10^{-02}	-0.33×10^{-03}
AAD% on ρ	0.94×10^{-01}	0.79×10^{-01}	0.82×10^{-01}
MD% on ρ	0.22	0.23	0.25

[a] AD, average deviation; AAD, absolute average deviation; MD, maximum deviation.

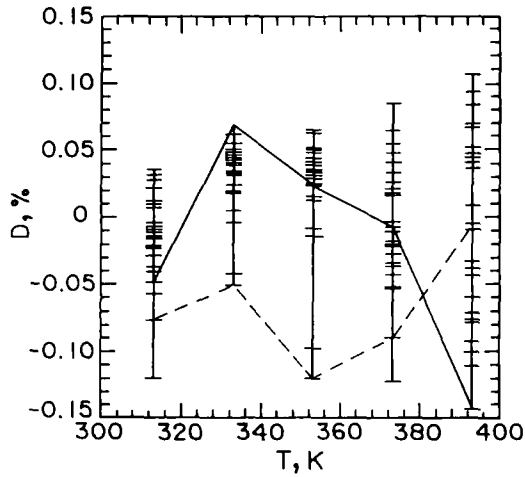

Fig. 4. Deviations in values of sound speed calculated from Eq. (3) versus experimental data for mixture b. (——) Maximum pressure; (---) minimum pressure.

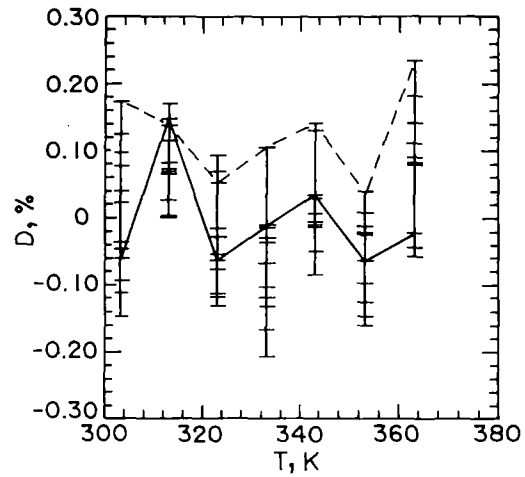

Fig. 5. Deviations in values of density calculated from Eq. (3) versus experimental data [1] for mixture b. (——) Maximum pressure; (---) minimum pressure.

Table VIII. Isentropic Compressibilities of Mixture a

	β_S (GPa)$^{-1}$ at T (K)			
P (MPa)	313.15	333.15	353.15	373.15
70	0.517	0.565	0.614	0.666
68	0.523	0.571	0.622	0.675
66	0.529	0.579	0.630	0.685
64	0.535	0.586	0.639	0.695
62	0.541	0.593	0.648	0.705
60	0.548	0.601	0.657	0.716
58	0.555	0.609	0.667	0.727
56	0.562	0.618	0.676	0.739
54	0.569	0.626	0.686	0.751
52	0.576	0.635	0.697	0.763
50	0.584	0.644	0.708	0.776
48	0.591	0.653	0.719	0.790
46	0.600	0.663	0.731	0.804
44	0.608	0.673	0.743	0.819
42	0.617	0.684	0.756	0.834
40	0.625	0.695	0.769	0.850
38	0.635	0.706	0.783	—
36	0.644	0.718	0.797	—
34	0.654	0.730	0.812	—
32	0.664	0.743	0.828	—
30	0.675	0.756	0.844	—
28	0.686	0.770	0.862	—
26	0.698	0.784	0.880	—
24	0.710	0.800	0.899	—
22	0.722	0.816	0.919	—
20	0.736	0.832	0.940	—
18	0.749	0.850	0.962	—
16	0.764	0.868	0.986	—
14	0.779	0.887	1.011	—
12	0.794	0.908	1.037	—
10	0.811	0.930	1.065	—
8	0.828	0.952	1.096	—
6	0.847	0.977	1.128	—
5	0.856	0.990	1.145	—
4	0.866	1.003	—	—

Table IX. Isentropic Compressibilities of Mixture b

	β_S (GPa)$^{-1}$ at T (K)				
P (MPa)	313.15	333.15	353.15	373.15	393.15
70	0.647	0.716	0.789	0.867	0.950
68	0.656	0.728	0.803	0.883	0.969
66	0.666	0.739	0.817	0.899	0.989
64	0.676	0.751	0.831	0.917	1.010
62	0.686	0.764	0.846	0.935	1.031
60	0.697	0.777	0.862	0.954	1.054
58	0.708	0.791	0.879	0.974	1.078
56	0.720	0.805	0.896	0.995	1.104
54	0.732	0.820	0.914	1.017	1.130
52	0.744	0.835	0.933	1.040	1.159
50	0.758	0.851	0.953	1.064	1.188
48	0.771	0.868	0.974	1.090	1.220
46	0.785	0.886	0.996	1.117	1.254
44	0.800	0.904	1.019	1.146	1.289
42	0.816	0.924	1.043	1.177	1.328
40	0.832	0.944	1.069	1.209	1.369
38	0.849	0.966	1.097	1.244	1.412
36	0.867	0.989	1.126	1.281	1.460
34	0.885	1.013	1.157	1.320	1.511
32	0.905	1.039	1.190	1.363	1.566
30	0.926	1.066	1.225	1.409	1.626
28	0.948	1.095	1.263	1.458	1.692
26	0.971	1.126	1.303	1.512	1.763
24	0.996	1.158	1.347	1.571	1.843
22	1.022	1.194	1.394	1.635	1.931
20	1.050	1.232	1.446	1.706	—

and average absolute deviations, it will be noted that the equation does not generate any systematic error in the prediction of either of the two properties.

Used by extension in the high-pressure interval (40–70 MPa), the model enabled us to complete the unavailable experimental density data. Thus the groups of curves for speed of sound were plotted as a function of the density, as shown in Fig. 6 for mixture b. One will observe the perfect

Table X. Isentropic Compressibilities of Mixture c

	β_S (GPa)$^{-1}$ at T (K)				
P (MPa)	313.15	333.15	353.15	373.15	393.15
70	0.616	0.683	0.754	0.830	0.911
68	0.624	0.693	0.767	0.844	0.929
66	0.633	0.704	0.779	0.860	0.947
64	0.642	0.715	0.792	0.875	0.965
62	0.651	0.726	0.806	0.892	0.985
60	0.660	0.737	0.820	0.909	1.005
58	0.670	0.750	0.834	0.926	1.027
56	0.680	0.762	0.850	0.945	1.049
54	0.691	0.775	0.866	0.964	1.073
52	0.702	0.789	0.882	0.985	1.098
50	0.713	0.803	0.900	1.006	1.124
48	0.725	0.817	0.918	1.029	1.152
46	0.737	0.833	0.937	1.053	1.182
44	0.750	0.849	0.957	1.078	1.213
42	0.763	0.866	0.979	1.104	1.246
40	0.777	0.883	1.001	1.132	1.281
38	0.792	0.902	1.024	1.162	1.319
36	0.807	0.921	1.049	1.194	1.359
34	0.823	0.942	1.075	1.227	1.403
32	0.839	0.963	1.103	1.263	1.449
30	0.857	0.986	1.133	1.302	1.499
28	0.875	1.010	1.165	1.343	1.554
26	0.894	1.036	1.198	1.388	1.613
24	0.915	1.063	1.234	1.436	1.678
22	0.936	1.092	1.273	1.488	1.749
20	0.959	1.123	1.315	1.545	1.827
18	0.983	1.156	1.360	1.607	1.914
16	1.009	1.191	1.409	1.675	2.012
14	1.036	1.229	1.462	1.751	2.121
12	1.066	1.270	1.520	—	—
10	1.097	—	—	—	—

regularity of the group of curves, for both temperature and pressure variations. As the equation of state is adapted through parameters b_1, b_2,..., c_4, γ, and β, for each system studied, we extended exploitation of the procedure to the calculation of isothermal and isentropic compressibility coefficients for the three ternary mixtures. The values generated by the procedure are presented together in Tables VIII to XIII, and Figs. 7 and 8

Table XI. Isothermal Compressibilities of Mixture a

	β_T (GPa)$^{-1}$ at T (K)			
P (MPa)	313.15	333.15	353.15	373.15
70	0.636	0.684	0.734	0.788
68	0.643	0.692	0.744	0.800
66	0.651	0.701	0.755	0.812
64	0.659	0.710	0.766	0.824
62	0.667	0.720	0.777	0.837
60	0.676	0.730	0.788	0.850
58	0.684	0.740	0.800	0.864
56	0.693	0.750	0.812	0.878
54	0.703	0.761	0.825	0.893
52	0.712	0.773	0.838	0.908
50	0.722	0.784	0.851	0.924
48	0.732	0.796	0.865	0.941
46	0.743	0.809	0.880	0.958
44	0.754	0.821	0.895	0.976
42	0.765	0.835	0.911	0.995
40	0.777	0.849	0.928	1.015
38	0.789	0.863	0.945	—
36	0.801	0.878	0.963	—
34	0.814	0.894	0.982	—
32	0.828	0.910	1.002	—
30	0.842	0.927	1.022	—
28	0.856	0.945	1.044	—
26	0.872	0.964	1.067	—
24	0.888	0.983	1.091	—
22	0.904	1.004	1.116	—
20	0.921	1.025	1.143	—
18	0.940	1.048	1.171	—
16	0.959	1.071	1.201	—
14	0.979	1.097	1.233	—
12	1.000	1.123	1.267	—
10	1.022	1.151	1.303	—
8	1.045	1.181	1.342	—
6	1.070	1.213	1.383	—
5	1.082	1.230	1.405	—
4	1.096	1.247	—	—

Table XII. Isothermal Compressibilities of Mixture b

	β_T (GPa)$^{-1}$ at T (K)				
P (MPa)	313.15	333.15	353.15	373.15	393.15
70	0.745	0.816	0.893	0.976	1.066
68	0.756	0.830	0.910	0.995	1.088
66	0.768	0.844	0.926	1.014	1.111
64	0.780	0.858	0.943	1.035	1.136
62	0.792	0.874	0.961	1.056	1.161
60	0.806	0.889	0.980	1.079	1.188
58	0.819	0.906	1.000	1.102	1.216
56	0.833	0.923	1.020	1.127	1.246
54	0.848	0.941	1.042	1.153	1.278
52	0.863	0.959	1.064	1.181	1.311
50	0.879	0.979	1.088	1.210	1.347
48	0.896	0.999	1.113	1.240	1.384
46	0.913	1.021	1.140	1.273	1.424
44	0.932	1.043	1.167	1.307	1.467
42	0.951	1.067	1.197	1.344	1.513
40	0.971	1.092	1.228	1.383	1.562
38	0.992	1.118	1.261	1.412	1.614
36	1.014	1.146	1.296	1.469	1.671
34	1.037	1.176	1.334	1.517	1.732
32	1.061	1.207	1.374	1.568	1.799
30	1.087	1.240	1.416	1.624	1.872
28	1.115	1.276	1.462	1.684	1.952
26	1.144	1.313	1.512	1.749	2.039
24	1.174	1.354	1.566	1.821	2.137
22	1.207	1.397	1.624	1.899	2.245
20	1.242	1.444	1.687	1.986	—

illustrate the dependency of these coefficients on temperature and pressure conditions. The $\beta_S(T)$ graphs show the linear dependency of the compressibility coefficient with respect to temperature; a similar behavior was observed in the case of natural gases [15], at high pressures. As for the degree of accuracy of evaluation of these properties, it can reasonably be expected that isentropic compressibility is defined to within better than 0.4%.

Table XIII. Isothermal Compressibilities of Mixture c

	β_T (GPa)$^{-1}$ at T (K)				
P (MPa)	313.15	333.15	353.15	373.15	393.15
70	0.723	0.794	0.869	0.951	1.039
68	0.734	0.807	0.884	0.968	1.060
66	0.745	0.819	0.900	0.987	1.082
64	0.756	0.833	0.916	1.006	1.104
62	0.768	0.847	0.932	1.025	1.128
60	0.780	0.861	0.949	1.046	1.153
58	0.792	0.876	0.967	1.068	1.179
56	0.805	0.892	0.986	1.090	1.206
54	0.818	0.908	1.006	1.114	1.235
52	0.832	0.925	1.026	1.139	1.265
50	0.847	0.942	1.048	1.165	1.297
48	0.861	0.961	1.070	1.193	1.331
46	0.877	0.980	1.094	1.222	1.367
44	0.893	1.000	1.119	1.253	1.405
42	0.910	1.021	1.145	1.285	1.445
40	0.928	1.043	1.173	1.320	1.489
38	0.947	1.067	1.202	1.357	1.535
36	0.966	1.091	1.233	1.396	1.585
34	0.987	1.117	1.266	1.437	1.638
32	1.008	1.144	1.301	1.482	1.696
30	1.031	1.173	1.338	1.530	1.758
28	1.054	1.204	1.377	1.582	1.826
26	1.079	1.236	1.420	1.637	1.900
24	1.106	1.271	1.465	1.698	1.981
22	1.134	1.308	1.514	1.763	2.070
20	1.163	1.347	1.567	1.835	2.170
18	1.195	1.390	1.624	1.914	2.280
16	1.228	1.435	1.687	2.001	2.404
14	1.264	1.484	1.755	2.097	2.544
12	1.303	1.538	1.830	—	—
10	1.344	—	—	—	—

5. CONCLUSION

As we mentioned in Section 1, it is particularly important when simulating the behavior of petroleum fluids to possess information on the variations of the compressibility coefficients β_S and β_T; the usefulness of such information is even more evident if they cover extensive pressure and temperature ranges. It should be stressed that it is accepted in petroleum engineering that the thermophysical phenomena which occur at the level of

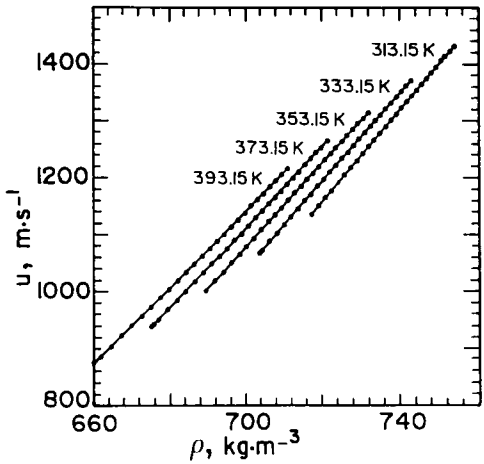

Fig. 6. Speed of sound in mixture b as a function of density.

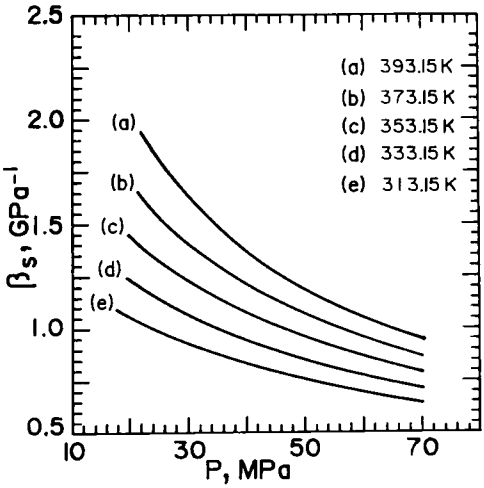

Fig. 7. Calculated isentropic compressibility in mixture b as a function of temperature.

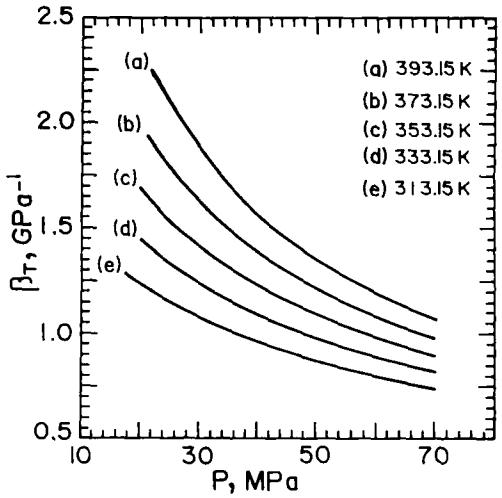

Fig. 8. Calculated isothermal compressibility in mixture b as a function of temperature.

the reservoirs themselves involve isothermal processes, whereas the decompression or compression processes which these fluids undergo in turboexpanders or compressors are essentially isentropic in nature.

Direct measurement of coefficients β_S and β_T up to high pressures (in the sense of gases and liquids) is not a common undertaking. This is why indirect evaluation through speed of sound and density measurements is so valuable, because of the greater experimental accessibility. This evaluation method enabled us to determine the compressibility coefficients for ternary mixtures in the liquid state but formed of pure components which are normally liquid (C_{16}) and gaseous (C_1 and CO_2). Such information on mixtures with this specific feature, connected with the simultaneous presence of substances with very low or very high compressibilities, is particularly rare. They are, however, very useful because they are characteristic of the fluids naturally present in deep geological strata.

ACKNOWLEDGMENTS

The authors wish to thank F. Montel for his highly appreciated assistance. They are also indebted to the Société ELF AQUITAINE for financial support.

REFERENCES

1. J. L. Daridon, H. Saint-Guirons, B. Lagourette, and P. Xans, *Ber. Bunsenges. Phys. Chem.* **97**:246 (1993).
2. S. Ye, J. Alliez, B. Lagourette, H. Saint-Guirons, J. Arman, and P. Xans, *Rev. Phys. Appl.* **25**:555 (1990).
3. E. P. Papadakis, *J. Appl. Phys.* **35**:1474 (1964).
4. G. Malfait and D. Jerome, *Rev. Phys. Appl.* **4**:467 (1969).
5. J. Paureau, *Rev. Phys. Appl.* **10**:475 (1975).
6. G. S. Kell and E. Whalley, *J. Chem. Phys.* **62**:3496 (1975).
7. L. A. Davis and R. B. Gordon, *J. Chem. Phys.* **46**:2650 (1967).
8. M. J. P. Muringer, N. J. Trappeniers, and S. N. Biswas, *Phys. Chem. Liq.* **14**:273 (1985).
9. J. L. Daridon, B. Lagourette, and P. Xans, *Fluid Phase Equil.* **100**:269 (1994).
10. R. L. Mills, D. H. Liebenberg, and J. C. Bronson, *J. Chem. Phys.* **63**:1198 (1975).
11. R. L. Mills, D. H. Liebenberg, J. C. Bronson, and L. C. Schmidt, *J. Chem. Phys.* **66**:3076 (1977).
12. R. L. Mills, D. H. Liebenberg, and J. C. Bronson, *J. Chem. Phys.* **68**:2663 (1978).
13. M. Benedict, G. B. Webb, and L. C. Rubin, *J. Chem. Phys.* **8**:334 (1940).
14. B. I. Lee and M. G. Kesler, *AIChE J.* **21**:510 (1975).
15. P. Labes, J. L. Daridon, B. Lagourette, and H. Saint-Guirons, *Int. J. Thermophys.* **15**:803 (1994).
16. B. Lagourette, J. L. Daridon, J. F. Gaubert, and P. Xans, *J. Chem Thermo.* **26**:1051 (1994).
17. B. Lagourette, J. L. Daridon, J. F. Gaubert, and H. Saint-Guirons, *J. Chem Thermo.* **27**:259 (1995).
18. S. Ye, B. Lagourette, J. Alliez, H. Saint-Guirons, P. Xans, and F. Montel, *Fluid Phase Equil.* **74**:157 (1992).
19. S. Ye, B. Lagourette, J. Alliez, H. Saint-Guirons, P. Xans, and F. Montel, *Fluid Phase Equil.* **74**:177 (1992).
20. A. L. Badalyan, N. F. Otpuschennikov, and U. S. Shoytov, *Izv. Akad. Nauk. Arm. USSR Fiz* **5**:448 (1970).
21. J. W. M. Boelhouwer, *Physica* **34**:484 (1967).
23. J. H. Dymond, J. Robertson, and J. D. Isdale, *Int. J. Thermophys.* **2**:133 (1981).